Shock Waves (2003) 12: 457–468
Digital Object Identifier (DOI) 10.1007/s00193-003-0186-1

Shock Waves

Detonation driver for enhancing shock tube performance

F.K. Lu, D.R. Wilson

Aerodynamics Research Center, Mechanical and Aerospace Engineering Department, University of Texas at Arlington, Arlington, TX 76019–0018, USA

Received 26 April 2002 / Accepted 23 December 2002
Published online 28 April 2003 –

Abstract. The development of a shock-induced detonation driver for enhancing the performance of a shock tube is described. The detonation wave is induced by the expansion of helium or air. Various gaseous fuel–oxidizer combinations are examined. This method produces a detonation wave which propagates downstream that transitions into a shock wave in the driven section. High-enthalpy flows with a maximum total temperature of 4200 K and a maximum total pressure of 34 atm in the driven tube are achieved. The problems of achieving the so-called perfectly-driven mode as well as those of inadequate fuel–oxidizer mixing are discussed.

Key words: Shock tube, Detonation driver, High enthalpy

1 Introduction

Historically, a large number of methods have been used to improve the performance of shock tubes and shock tunnels (Warren and Harris, 1970). One method is to fill the driver section with a light gas such as helium. Another is to increase the temperature of the driver gas by use of a heater. In both of these methods, the improved performance is achieved by a higher speed of sound than if cold air is used. In the first case, the speed of sound in helium is higher than air because of its lower molecular weight. In the latter, the speed of sound is increased by raising the gas temperature. The higher sound speed results in a lower driver-to-driven tube pressure ratio p_4/p_1 required to generate a given incident shock Mach number in the driven tube, or a higher incident shock Mach number for the same value of p_4/p_1.

Although both of the abovementioned approaches are well established, there are a number of disadvantages associated with them. Both require high pressure pumps and plumbing. Helium is expensive and large amounts must be used to pressurize the driver tube. Helium's higher specific heat ratio also reduces the advantages somewhat. If the driver tube is to be heated, the tube must be designed to withstand high pressure under high temperatures, adding to the construction costs. The heater also adds to the cost and it must be designed to heat uniformly because hot spots in the driver can cause unpredictable and dangerous driver tube failure. Thermal fatigue may, in fact, limit the useful life of the tube.

For quite some time, the free-piston driving technique, first proposed by Stalker (1967), has been used to achieve some of the highest enthalpies, culminating in the X3 at the University of Queensland, Brisbane, Australia (Morgan 2000), the HEG in Göttingen, Germany (Hannemann and Beck, 2002), and the largest known facility, the HIEST in Kakuda, Japan (Itoh, 2002). The free-piston technique involves compressing the driver gas by a heavy piston accelerated to nearly sonic speed. The piston compresses the gas ahead of it to achieve high values of temperature and pressure. The operation of a free-piston shock tunnel, however, appears to be complicated, as a massive piston has to be accelerated rapidly and then must be stopped in a controlled manner.

Alternatively, a simpler approach to improve the performance of the shock tube uses a detonation driver, especially by using oxyhydrogen mixtures with helium dilution. Presently, the enthalpies achieved by detonation driver techniques are lower than those of free-piston drivers. Nonetheless, a combination of a detonation driver and an expansion tube has been shown to be capable of achieving extremely high enthalpies (Chue et al., 2002).

Benefits of using a detonable mixture as the driver gas are that the detonation achieves a high pressure, a high temperature, a low specific heat ratio and a high speed of sound. All of the above features can be shown theoretically to be capable of producing a high shock Mach number, thereby improving the shock tube's performance. A major drawback, however, is that the gaseous detonation products have high molecular weight compared to helium.

The initial pressure of the gaseous mixture in a detonation driver is quite low, being a few atmospheres, which eliminates the need for high pressure equipment. The high temperature is generated for a very short period so the driver structure is not exposed to prolonged heating. The

Correspondence to: F.K. Lu (e-mail: lu@mae.uta.edu)

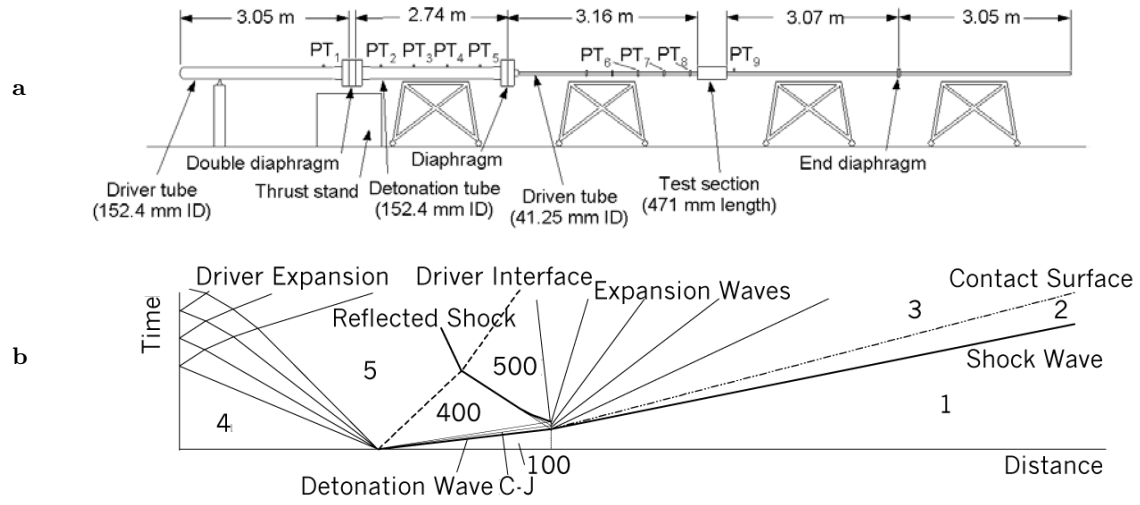

Fig. 1a,b. Shock-induced detonation driven shock tube: **a** schematic, **b** simplified wave diagram for specified geometry (thick line – shock or detonation wave, thin line – expansion wave, chain line – contact surface)

design is thus reduced primarily to one of pressure containment. Disadvantages are the dangers involved with the explosive mixture and, perhaps, the cost of an ignition source. The danger of the explosive mixture can be reduced by helium dilution. Helium dilution does not substantially degrade performance. Helium dilution actually allows control of the temperature generated in the driver. The molecular weight of the driver gas is reduced by helium addition, which improves performance, thereby mitigating the drawback mentioned in the above paragraph. The addition of helium slightly increases the energy required to cause a detonation. This enhances safety without significantly increasing the cost as only a small amount of helium is used compared to a pure helium driver (Olivier et al., 2002). Note that argon dilution is highlighted in Lu et al. (2000).

The detonation driver technique is not new and can be traced to early research by Bird (1957), and Coates and Gaydon (1965), amongst others. Due to the aforementioned advantages, the detonation driver has been reexamined lately. Reviews of recent developments can be found in Lu et al. (2000) and Olivier et al. (2002). Thus, only a brief background is provided here. Instead, the purpose of this paper is to report details that were left out in the reviews, specifically those of the performance of a shock-induced detonation driven shock tube.

2 Facility development

2.1 Shock-induced detonation principle

The detonation-driven shock tube can be operated in an upstream or a downstream mode (Lu et al., 2000; Olivier et al., 2002). In the former, the wave initiation source is located at the downstream end of the driver near the diaphragm. This uses the high pressure gas behind the detonation wave to rupture the diaphragm and initiate the incident shock wave in the driven tube. The inert shock formed in the combustible mixture develops into a detonation after a short induction process. If the initiation energy of the driver is large enough and the Mach number of the initiating shock wave is larger than the CJ Mach number of the combustible mixture, an overdriven detonation is produced which decays to CJ detonation. In passing, it may be noted that the issue of direct initiation is not immediately important in facility development unlike the issue of repeatability. Direct initiation and the issues related to deflagration-to-detonation transition have been the subject of much study such as, for example, the recent works by Nettleton (2002) and Thomas and Bambrey (2002). In our experience, the repeatability of a shock-induced detonation-driven shock tube is excellent, being primarily determined by the ability to control the diaphragm breakage process.

The detonation wave travels upstream and is then reflected from the closed end of the driver, generating extremely high pressures. Care has to be exercised that the high pressure does not exceed the structural limits of the driver. For example, a damping tube is used by Yu et al. (1992) to ensure structural integrity. The upstream mode yields a more uniform test flow albeit at a lower enthalpy than that of a downstream mode with the same initial conditions. In the downstream or forward propagation mode, the gas momentum is available to yield the extra performance. However, as indicated in the wave diagram of Fig. 1b, the Taylor rarefaction following the detonation wave in between regions 100 and 400 can produce a non-uniform test flow.

The non-uniform test flow can be somewhat overcome by not using an electric igniter but by using a shock wave to initiate the detonation. For the configuration shown in Fig. 1a, high-pressure air or helium fills the driver tube, while a stoichiometric oxyhydrogen mixture fills the detonation tube at pressures of 1–9 atm. The driven tube is filled with the test gas (air, say) at low pressure. Rup-

turing the double diaphragm causes a shock wave to be induced in the detonation tube. This shock rapidly transitions into a detonation wave propagating to the right. The high pressure behind this detonation wave ruptures the diaphragm separating the detonation and driven tubes, to initiate flow in the driven tube. A quasi-uniform flow region 2 exists behind the shock, to be followed by an expansion region 3.

As mentioned above, the Taylor rarefaction following the detonation wave can cause a non-uniform "pumping" of the flow in the driven tube. It is possible, in certain circumstances, to eliminate the Taylor rarefaction, to produce a so-called perfectly driven mode (Lu et al., 2000). In the perfectly driven mode, therefore, an adequately steady flow can be obtained. If Taylor rarefaction exists, the under-driven or weak (in the parlance of detonation researchers) mode is obtained. Finally, it is also possible to have an over-driven (or strong) mode. Unfortunately, the terminology can be confusing between practitioners of shock tunnel techniques and detonation physics researchers, who use the terms under, perfectly and over-driven for two different concepts. In this paper, the practice is that of the former.

2.2 Facility design and performance analysis

The downstream mode was chosen for further development due to the higher enthalpies that can be obtained compared to the upstream mode. `TEP`,[1] a Windows™ version of the NASA `CEA`[2] code (Gordon and McBride, 1976) is used for design and performance analysis calculations of the detonation-driven shock tube. This code can be used for real-gas calculations of gasdynamic processes, such as Chapman–Jouguet (CJ) detonation waves, and shock tube performance. A quasi-one-dimensional flow model is assumed, and real gas calculations based on both equilibrium and frozen flow models are available. All of the calculations presented in this paper assume equilibrium flow.

`TEP` is first used to calculate detonation tube performance for stoichiometric oxyhydrogen mixtures for a range of initial pressures and with different amounts of helium dilution. A one-dimensional, perfect gas code is used to calculate the driven-tube pressure ratio p_2/p_1 and shock speed u_s as a function of the shock tube pressure ratio p_4/p_1. (Prior comparisons with real gas codes indicate that p_2/p_1 and u_s are generally within 5% of real gas results.) The `TEP` code is then used to calculate the temperature ratio across the incident shock wave using the perfect-gas value of u_s.

Figure 2 displays the predicted performance of the detonation driver, with an area reduction of 14.5 (Alpher and White, 1958). The performance envelope is obtained for a stoichiometric oxyhydrogen mixture at initial pressures of 1–9 atm and a driven tube filled with air at initial pressures of 0.063–10 atm. The gas temperatures are 300 K. Also included are the performance maps of cold air and cold helium drivers, filling the driver tube up to its maximum rating of 408 atm. Figure 2 shows that the detonation driver enhances the performance of the shock tunnel very significantly.

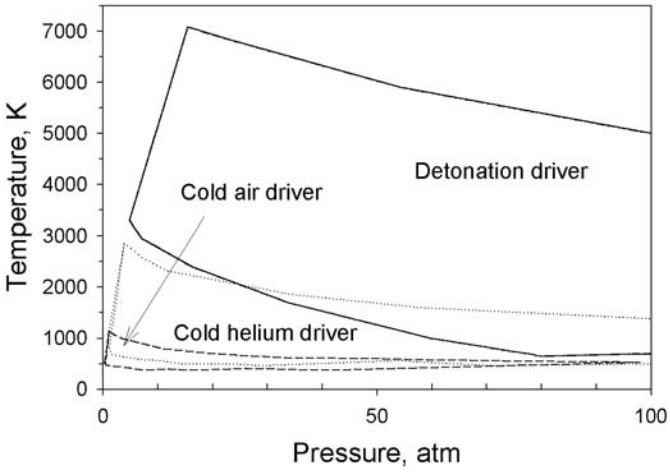

Fig. 2. Calculated performance of the shock tube with a detonation driver and a 14.7:1 detonation-to-driver tube area ratio (axes are the stagnation conditions in the driven tube)

3 Facility description

With the promise of enhanced performance, an existing shock tunnel was modified into a detonation-driven shock tube as shown schematically in Fig. 1a. The driver section has a bore of 152.4 mm and a length of 3.05 m. The detonation section also has a bore of 152.4 mm but is 2.74 m long. Both tube sections are rated for a pressure of 408 atm. These two tubes are separated by a double-diaphragm section. The diaphragms are made from 3.42 or 2.66 mm hot-rolled 1008 steel plates, scored to various depths in a cross pattern. The scored sides face downstream.

The detonation tube has two ports for filling and purging. Hydrogen and oxygen are injected through separate lines for safety. The detonation tube is evacuated through the hydrogen line to 0.02 atm. The hydrogen line is also used for venting the tube after a run or for purging the combustible mixture if there is an abort. Helium and purge air are injected through the oxygen line.

The detonation and driven sections are separated by a 0.35 mm thick mylar diaphragm. A 9 m driven tube with a 40 mm bore is installed to produce a 14.5:1 area reduction at the primary diaphragm. The pressure rating of the driven tube is 188 atm. The test section, is located 3.16 m from the primary diaphragm location and has an overall length of 471 mm. It comprises an electrical conductivity channel 115.9 mm long, with 152.4 mm long lexan insulators and 25 mm thick end flanges on either side. Another section of the driven tube, 6.12 m long, is installed downstream of the test section to prevent wave reflections from the open end from interfering with the test flow. A 0.35 mm thick mylar diaphragm is inserted at 3.07 m down-

[1] Thermodynamic Equilibrium Program
[2] Chemical Equilibrium with Applications

stream of the test section to contain the initial driven tube gas.

The filling and purging systems for the driver and driven tubes are relatively simple since no reactive gases are used there. Separate vacuum systems are used to evacuate these tubes to 0.02 atm. The driver tube is filled to the desired pressure with either air or helium. In case of an abort, the tube can be vented. Similarly, the driven tube is evacuated before being filled with dry air. The double diaphragm section separating the driver and detonation tubes is filled with air at about half the pressure of the driver tube. A run is initiated by releasing the pressure in the double diaphragm section. This causes the upstream diaphragm to rupture, which immediately causes the downstream diaphragm to also rupture. The high-pressure gas in the driver tube expanding into the detonation section propagates a shock wave which rapidly transitions into a detonation wave, as depicted in Fig. 1b which features an under-driven mode of operation. The wave that propagates downstream through the detonation tube transitions to a CJ detonation wave. Unfortunately, the pressure transducers are not located sufficiently far upstream to detect this transition and it is estimated that transition occurs within 0.2 m. The propagating detonation wave impinges the thin downstream diaphragm to rupture it. The area reduction causes part of the wave to be reflected. This partial reflection serves to trap high-pressure gas in a fashion similar to a reflected shock tunnel and serves to alleviate attenuation from the Taylor rarefaction, thereby prolonging the duration of uniform flow within the driven tube. Jiang et al. (1999, 2002) have further studied this technique of increasing the run time and flow uniformity through the use of "cavity rings." Finally, at the end of a successful run, the end diaphragm is blown away and the entire shock tube is vented.

4 Instrumentation

The driver tube is instrumented with a flush-mounted pressure transducer PT_1 while the detonation tube is instrumented with four flush-mounted pressure transducers, PT_2–PT_5 (PCB model 111A22, full-scale range of 680 atm, rise time of 2 μs and time constant of 1000 s) for monitoring the behavior of the detonation wave (Fig. 1a). The transducers are located at 0.495, 1.08, 1.66 and 2.25 m upstream of the mylar diaphragm separating the detonation and driven tubes. An MKS model 127A Baratron pressure transducer, with a maximum pressure rating of 13.1 atm, is used when filling the detonation tube using the method of partial pressures. It is also used to provide an initial pressure reading for setting the PCB transducers. The Baratron transducer is isolated from the detonation tube just before a run to prevent damage by the propagating detonation wave.

The driven section is instrumented with two flush-mounted PCB model 111A23 transducers (PT_6 and PT_7 in Fig. 1a) which have a full-scale pressure range of 340 atm, rise time of 2 μs and a time constant of 500 s. These transducers, located upstream of the test section at 2.146 and 2.604 m respectively downstream of the secondary diaphragm location, are used primarily for shock speed measurements. Two other PCB transducers (model 111A23 or 111A24 depending upon the conditions in the driven tube) are installed at PT_8 and PT_9, located at 3.061 and 3.416 m respectively downstream of the secondary diaphragm location. The model 111A24 transducers have a full-scale range of 68 atm, a rise time of 2 μs and a time constant of 100 s. The four transducers monitored the transient conditions in the driven section during a run. The initial pressure in the driven tube is also measured by an MKS model 127A Baratron pressure transducer but with a maximum pressure range of 1.3 atm. This transducer provides an accurate measurement of the initial driven tube pressure as well as serving to initialize the dynamic PCB transducers. Just like the above Baratron transducer, this Baratron transducer is isolated from the driven tube just before a run to prevent damage by the propagating shock wave.

Data are recorded simultaneously by a multi-channel data acquisition system at 100 kHz/channel. The data acquisition system is triggered externally. A soft, thin wire is mounted on the end diaphragm of the driven tube. Triggering occurred when the end diaphragm and the wire are broken by the shock or detonation wave generated in the driven tube. The data acquisition system is capable of recording pre-trigger data. The required amount of pre-trigger data is determined by consideration of the shock and detonation wave propagation in the shock tube. Further, time-of-flight (TOF) calculations using data between two transducers are used to obtain the wave propagation speeds. The wave speed provides an important indication of the properties of the detonation wave, primarily in determining the transition to a fully-developed CJ wave.

Initial gas pressures in the driver and detonation tubes (p_4 and p_{100}) are determined to an accuracy of ±1%. Due to leaks in the test section, the initial pressure p_1 in the driven tube can only be determined to an accuracy of ±16.1%, which resulted in an accuracy of ±5% in p_2. Initial gas temperatures are accurate to ±1 K. The mixture composition in the detonation tube (using the method of partial pressures) is accurate to ±1%. Most of the mixtures were stoichiometric oxyhydrogen, although some tests were made with stoichiometric mixtures of hydrogen/air and propane/oxygen. Wave velocities, obtained from TOF measurements, are accurate ±2–3%. Due to the large spacing between the transducers, the wave velocity should be regarded as an average value between the respective transducer pairs. For the purpose of understanding wave processes in the detonation and driven tubes, the deduced velocities are sufficient.

5 Results and discussion

5.1 Arc initiation

The detonation was at first triggered by an electric arc of about 3 J and, therefore, the driver section shown in Fig. 1a is not used. An example of the detonation tube

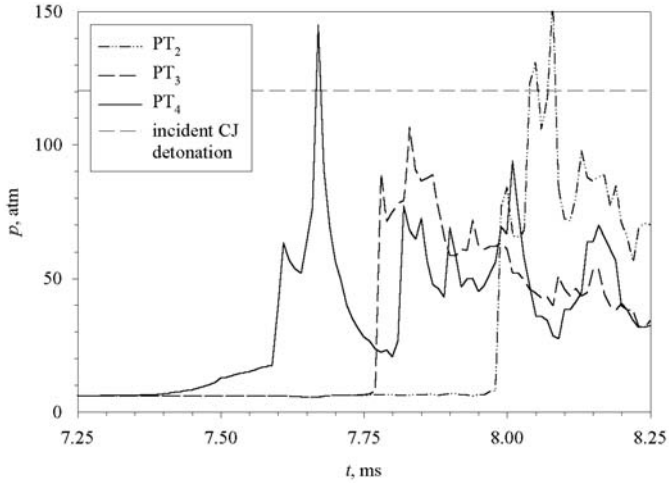

Fig. 3. Pressure trace for a stoichiometric oxyhydrogen mixture, initial pressure = 6.0 atm; arc ignition, energy ≈ 3 J

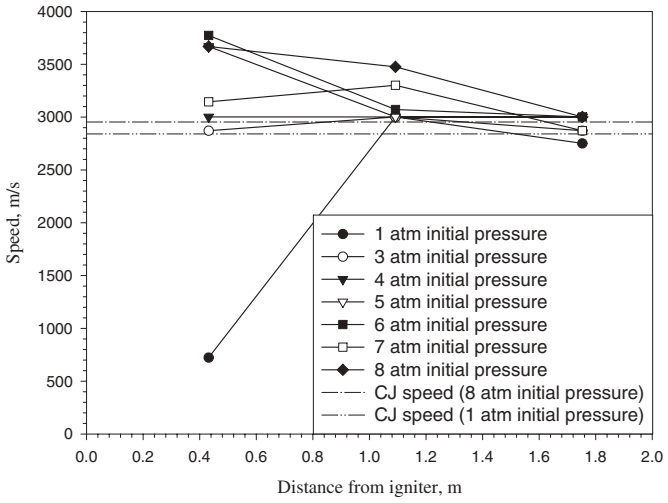

Fig. 4. Wave speed for a stoichiometric oxyhydrogen mixture at different initial pressures due to arc ignition (lines added for visual aid)

pressure history is shown in Fig. 3 for a stoichiometric reactant mixture at an initial pressure of 6 atm. The igniter is located on the sidewall of the detonation tube, 228.6 mm from the mylar diaphragm, that is, it is just upstream of PT_5. Thus, the detonation wave propagates upstream. The transducer closest to the igniter shows some precompression ahead of the detonation wave. Nonetheless, TOF calculations indicate the detonation wave reaches or exceeds the CJ speed (Fig. 4). The peak pressure levels (not shown) are also in reasonable agreement with the CJ level. Deflagration-to-detonation transition occurs within 0.4 m (length-to-diameter ≈ 2.6) for all initial pressures above 1 atm.

Although, a CJ detonation wave is eventually achieved in the detonation tube, arc-induced detonation proves inadequate for facility development for two primary reasons. First is the rapid decay in pressure following passage of the detonation wave caused by the Taylor rarefaction. Second is the inability to directly initiate a CJ detonation with low initial reactant pressures, as can be seen in the 1 atm data in Fig. 4. Despite the poor spatial resolution of the data, the indication is that the deflagration-to-detonation (DDT) transition occurs between 1 and 1.7 m from the igniter for the 1 atm case, a distance longer than desirable. To improve shock tube performance, the shock-induced detonation technique proposed by Bakos et al. (1996) was adopted. Bakos et al. (1996) reported a short and consistent DDT distance which is important for repeatability. Moreover, using shock-induced detonation, the expansion of the high-pressure gas from the driver tube can ideally eliminate the Taylor rarefaction, resulting in a sustained CJ pressure level behind the detonation wave. The development of shock-induced detonation is discussed next.

5.2 Shock-induced detonation

Detonation tube pressures corresponding to the underdriven mode of operation, in which the Taylor rarefaction wave is only partly eliminated, are shown in Fig. 5.

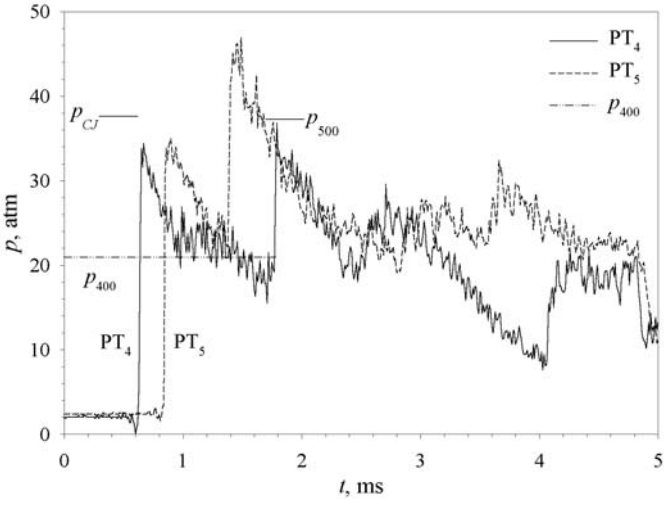

Fig. 5. Detonation tube pressure traces for a stoichiometric oxyhydrogen mixture at an initial pressure of 2 atm with shock-induced detonation using an air driver (p_4 = 219 atm and T_4 = 300 K)

The detonation tube is filled with a stoichiometric oxyhydrogen mixture at 2 atm. High-pressure air is used to initiate a shock-induced detonation. In Fig. 5, the first peak is due to the incident detonation wave and the second to the wave reflected from the downstream end of the detonation tube. The detonation speed is calculated by a TOF method from the distance between the two transducers and the propagation time of the incident wave. From the speed and the distance between the transducers and double diaphragm section, the instant that the double diaphragm broke is estimated. The abscissa in Fig. 5 is the time delay after the estimated instant of diaphragm breakage.

`TEP` is used to calculate conditions in the detonated gas for given initial conditions. From the conservation equa-

tions for continuity, momentum, and energy, and the constraint that $u_{CJ} = a_{CJ}$, TEP yields the CJ parameters and also the state and composition of the detonation products. The detonation wave velocity u_d is dependent only on the initial conditions of the detonation mixture. However, incomplete mixing of fuel and oxidizer is thought to cause the experimental value of u_d to be different from the theoretical speed u_{CJ}. Nonetheless, if the difference between the measured velocity and the CJ velocity is within 10%, it is assumed that detonation is achieved since this criterion clearly distinguishes the detonation wave from a propagating shock; the latter would travel at a much lower speed. (The procedure for estimating the experimental value of u_d is described below.) The CJ parameters calculated using TEP are corrected for incomplete mixing. An appropriate portion of fuel which produces the measured velocity is substituted with an equivalent amount of a nonreactive gas of the same molecular weight, such as a helium atom for a hydrogen molecule. The corrected p_{CJ} obtained by TEP is indicated in Fig. 5. It can be seen that the pressure transducer is unable to resolve the theoretical p_{CJ}.

The theoretical plateau pressure p_{400} behind the Taylor rarefaction is derived as follows. From the characteristic curve between regions 4 and 5,

$$p_4/p_5 = \left(1 + \frac{\gamma_4 - 1}{2}\frac{u_5}{a_5}\right)^{[2\gamma_4/(\gamma_4-1)]} . \quad (1)$$

Assuming isentropic expansion and a calorically perfect gas,

$$a_5/a_4 = (p_5/p_4)^{[(\gamma_4-1)/2\gamma_4]} .$$

Therefore, (1) becomes

$$(p_5/p_4)^{[(\gamma_4-1)/2\gamma_4]} = 1 - [(\gamma_4 - 1)/2]\, u_5/a_4 . \quad (2)$$

In the Taylor rarefaction that follows the detonation wave, the same characteristics give

$$\left(\frac{p_{400}}{p_{CJ}}\right)^{[(\gamma_{CJ}-1)/2\gamma_{CJ}]} = 1 - \frac{(\gamma_{CJ} - 1)}{2}\,\frac{u_{CJ} - u_{400}}{a_{CJ}} . \quad (3)$$

Since, between the contact surface,

$$p_5 = p_{400} \quad \text{and} \quad u_5 = u_{400}$$

from (2) and (3), the theoretical pressure in region 400 can be expressed as

$$p_{400}^{f(4)} + A\, p_{400}^{f(CJ)} + B = 0 \quad (4)$$

where

$$A = \frac{\gamma_4 - 1}{\gamma_{CJ} - 1}\,\frac{a_{CJ}}{a_4}\, p_{CJ}^{-f(CJ)}\, p_4^{f(4)}$$

$$B = \left[\frac{\gamma_4 - 1}{2}\,\frac{u_{CJ}}{a_4} - \frac{\gamma_4 - 1}{\gamma_{CJ} - 1}\,\frac{a_{CJ}}{a_4} - 1\right] p_4^{f(4)}$$

$$f(i) = (\gamma_i - 1)/2\gamma_i .$$

Equation (4) is not explicit, but from the CJ and initial driver conditions, the plateau pressure of region 400 can be obtained numerically. For a driver gas with a low molecular weight, such as helium or hydrogen, the plateau pressure p_{400} becomes large. The effect of the driver gas on shock tube performance will be discussed in Sect. 5.5. The pressure p_{400} calculated by (4) is indicated in Fig. 5 and listed in Table 1. Although it is hard to uniquely determine the experimental plateau pressure, Fig. 5 shows a good agreement with the theoretical value.

From (3), u_{400} is also calculated. This is the same value as u_5, the speed at the head of the expansion in the high-pressure driver. Therefore, the instances when the driver interface arrives at PT_4 and PT_5 are calculated as 3.61 and 4.88 ms, respectively. A slight modification of (2) yields

$$a_{400} = \frac{\gamma_4 - 1}{2}\, u_{400}\left[1 - \left(\frac{p_{400}}{p_4}\right)^{[(\gamma_4-1)/2\gamma_4]}\right]^{-1} . \quad (5)$$

Since the tail of the Taylor rarefaction advances at a speed of $(a_{400} + u_{400})$, the calculated arrivals of the rarefaction tail at PT_4 and PT_5 are 0.89 and 1.21 ms, respectively. In general, the measured detonation wave speeds in the detonation tube are within 10% of the CJ speed. A possible reason for the lower measured values in the driven tube is boundary-layer growth (Olivier et al., 2002).

5.3 Reflected and transmitted shocks

The detonation wave is reflected by the cross-sectional area change and the presence of a diaphragm between the detonation and driven tubes. Since the reflected shock propagates through region 400, the plateau pressure p_{400} $(= p_5)$ and the reflected shock speed govern the state of region 500. In order to apply normal shock relations to the conditions in region 400, the reflected shock speed is derived using the TOF method between PT_4 and PT_5. The shock routine in TEP is applied to yield $p_{500}, T_{500}, a_{500}$, u_{500} and γ_{500}.

For the example shown in Fig. 5, the theoretical values of p_{500} and T_{500} are listed in Table 1. The theoretical value of p_{500} is in reasonably good agreement with the measured peak pressure as indicated in Fig. 5. The peak pressure measured at PT_5 is somewhat higher than that at PT_4. The reason for the high pressure is that when the detonation wave arrives at the mylar diaphragm, the pressure behind the detonation wave is higher than p_{400} since it is not yet attenuated by the Taylor rarefaction. Therefore, as the detonation wave reflects and propagates through the gas at higher pressure, the post-shock pressure becomes temporarily higher than p_{500}. Due to progressive attenuation by the Taylor rarefaction, the reflected shock accelerates until it encounters the plateau pressure. The gas velocity after the reflected shock u_{500} is calculated to be -277 m/s, which means that the gas in region 500 is moving upstream. The pressure is attenuated by an expansion wave following the reflected shock.

The downstream propagating detonation wave in addition to being reflected is also partially transmitted into

Table 1. Example of initial conditions and calculated properties

Tube	Initial conditions			Calculated properties		
	Gas	Region	p, atm	Region	p, atm	T, K
Driver	Air	4	183	5	20.9	161
Detonation	$2H_2+O_2$	100	2.01	CJ	37.7	3630
				400	20.9	3390
				500	37.1	3790
Driven	Air	1	0.97	2	14.4	975

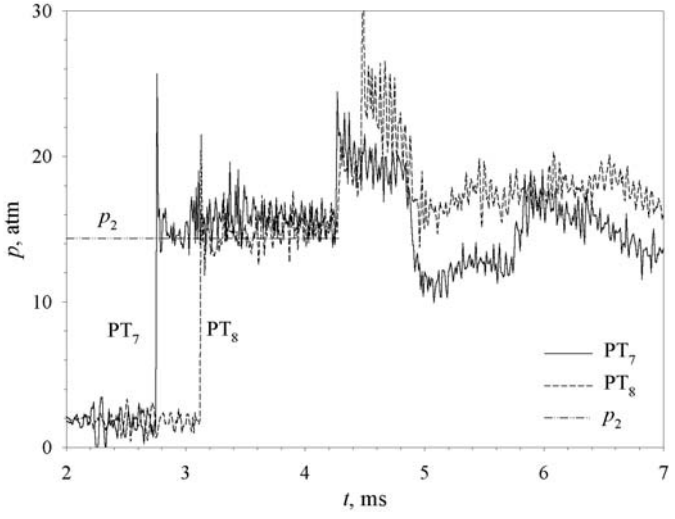

Fig. 6. Pressures in driven tube (air initially at 2 atm and 300 K)

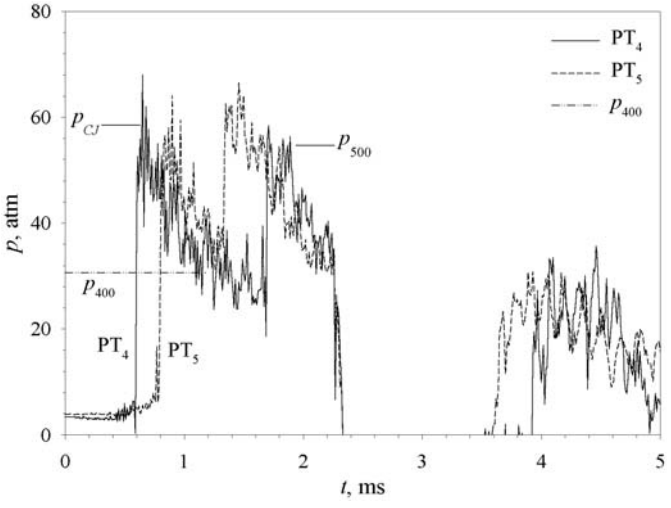

Fig. 7. Detonation pressures of oxyhydrogen at $p_{100} = 3$ atm with an air driver at 219 atm and 300 K – electromagnetic interference caused signal fallout between approximately 2.4 and 3.5 ms but does not affect interpretation of prior signal

the driven tube. Pressures recorded in the driven tube are shown in Fig. 6. The abscissa is the time from the estimated moment of primary diaphragm breakage. The flow in region 2 is supersonic with a Mach number of $M_2 = 1.57$. Thus, the second peak and dip after about 4.6 ms may be due to another shock and expansion wave behind the primary shock. The properties in region 2 are derived by the normal shock relations using the measured shock velocity u_s. The calculated pressure p_2 compares favorably with the measurements as indicated in Fig. 6.

5.4 Effect of reactants

Detonations are established in oxyhydrogen, hydrogen/air and propane/oxygen mixtures driven by air and helium. The effect of raising the initial pressure p_{100} of the reactants from 2 to 3 atm can be seen in a comparison of Fig. 7 with Fig. 5, both being under-driven cases. It is difficult to determine p_{CJ} from the data due to the onset of Taylor rarefaction and instrumentation limitations. Nonetheless, the pressure in the detonation products is increased by 50% for the same increase in p_{100} as required by theory. The detonation wave speed is calculated to be 2660 and 2780 m/s for $p_{100} = 2$ and 3 atm respectively. This indicates that the detonation velocities are not strongly dependent on initial pressure.

Figure 8 shows detonation pressure traces for a propane/oxygen mixture initially at 2 atm. This can also be compared with Fig. 5 for the same initial conditions except for a difference in mixture composition. For the propane/oxygen case, the detonation velocity is estimated as 2430 m/s, which is slower than in the oxyhydrogen case. However, it can be observed that the post-detonation pressure is larger. The peak pressure in the detonation wave for the propane/oxygen case is measured at 63 atm while that for the oxyhydrogen case is only 34.4 atm. Even though the instrumentation may not exactly resolve the peak pressures, the measurements are consistent with the higher predictions of p_{CJ} for the propane/oxygen case, the value of which is indicated in Fig. 8.

`TEP` provides the theoretical detonation velocities and post-detonation pressures for various initial conditions. As a summary, Fig. 9 shows the detonation velocity for stoichiometric mixtures of different reactant pairs at initial pressures of 0.5–4.0 atm. The velocities obtained in the experiments are generally lower than the calculated values except for the hydrogen/air cases, which are as much

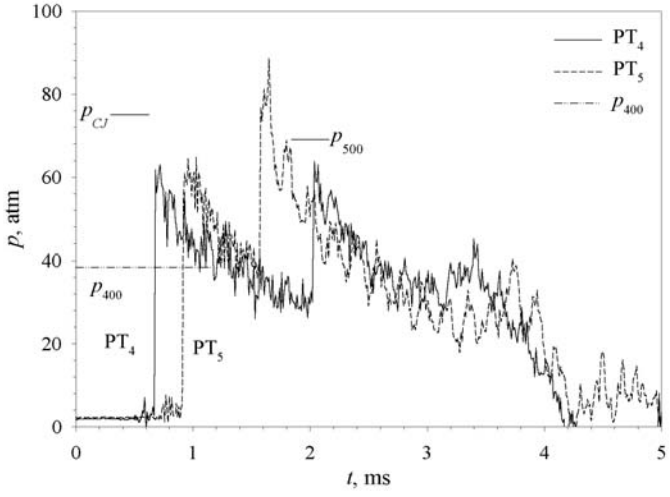

Fig. 8. Detonation pressures of propane/oxygen at $p_{100} = 2$ atm with an air driver at 219 atm and 300 K

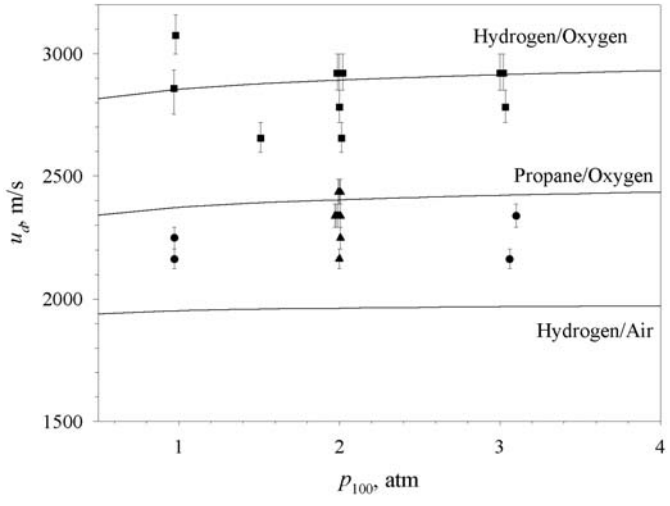

Fig. 9. Detonation velocity dependence on reactants (stoichiometric mixtures in all cases): TEP results are shown as lines, experimental values for hydrogen/oxygen are shown as squares, for propane/oxygen as triangles, and for hydrogen/air as circles (vertical error bars are due to the 10 μs temporal resolution)

as 20% higher. For the hydrogen/air case, it was thought that incomplete mixing may produce oxyhydrogen mixtures locally, resulting in the higher velocity.

Figure 10 compares the measured post-detonation pressure and the values calculated using TEP. The symbols denote the same mixtures as in Fig. 9. The experimental determination of p_{CJ} is difficult because of the rapid initial decay of pressure from its peak, von Neumann value. However, to compare the post-detonation pressure, the pressure is averaged over 0.1 ms after the peak to provide consistency in its evaluation. Thus, $\bar{p}_{CJ}$ is the averaged pressure assuming that it represents p_{CJ}. The experiments and calculations both indicate that the highest pressures are obtained with propane/oxygen mixtures. The measured pressure increases for large initial pressure. Moreover, the hydrogen/air cases show that most departures from the theoretical values are likely due to the incomplete mixing.

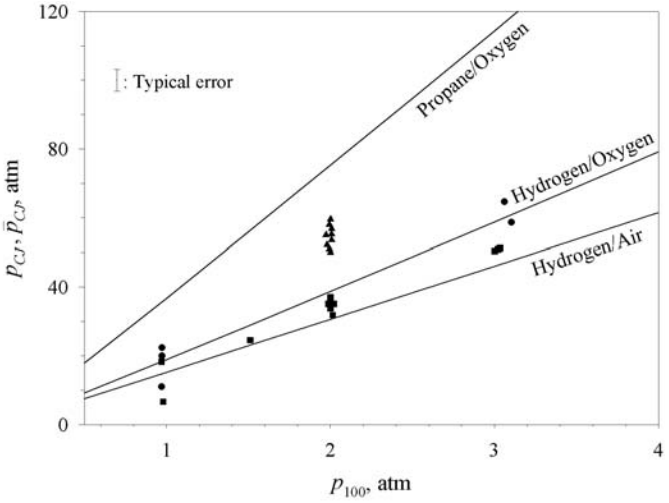

Fig. 10. CJ pressure dependence on reactants (stoichiometric mixtures in all cases): TEP results are shown as lines, experimental values for hydrogen/oxygen are shown as squares, for propane/oxygen as triangles, and for hydrogen/air as circles

5.5 Driver gas

The uniform region 400 of detonation products is determined by the state of the driver gas in region 4 and CJ parameters as indicated by (4). The equation implies that the attenuation of the detonation wave followed by the Taylor rarefaction determines p_{400} since the Taylor rarefaction exists to match the pressure of the expanding driver gas. For example, the theoretical plateau pressures when an air, helium or hydrogen driver is used to detonate a stoichiometric oxyhydrogen or hydrogen/air mixture initially at 2 atm and 300 K are shown in Fig. 11 as solid and dashed lines respectively. Note that while the figure shows a hydrogen driver, this approach is not used in the experiments. The CJ pressures are also shown as chain lines.

The calculations show that p_{400} increases with p_4. For a stoichiometric oxyhydrogen mixture, the strong Taylor rarefaction prevents p_{400} from reaching p_{CJ} with an air driver for the p_4 range considered here and only underdriven conditions are achieved. It can be noted that for hydrogen driving the stoichiometric oxyhydrogen mixture, the pressure of the hydrogen driver just balances the pressure at the rear of the detonation wave p_{CJ} at 185 atm, annihilating the Taylor rarefaction. In this perfectly driven mode, the full CJ pressure level can ideally be maintained behind the detonation wave. A further increase in p_4 causes the expanded driver gas pressure to be higher than the CJ pressure. This forces the detonation to travel faster than the CJ speed, resulting in an over-driven detonation. Taylor rarefaction does not exist in this case. Finally, since hydrogen is not used as a driver gas, none of the reported experiments achieved over-driven conditions

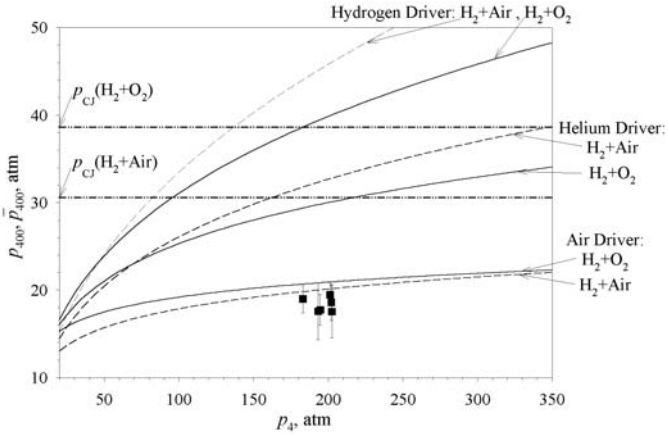

Fig. 11. Plateau pressures for air, helium, and hydrogen drivers (stoichiometric reactant mixtures at 2 atm and 300 K initial conditions)

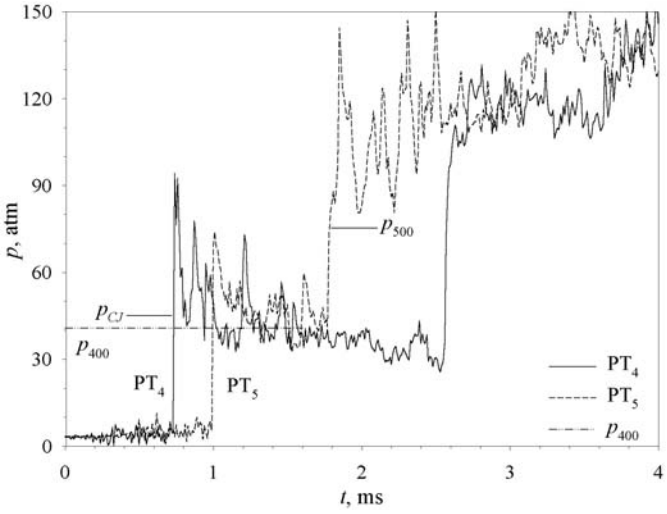

Fig. 12. Detonation pressures of oxyhydrogen at $p_{100} = 3$ atm with a helium driver at 219 atm and 300 K

and very few achieved nearly perfectly-driven conditions for the range of fill pressures attempted. For a stoichiometric hydrogen/air detonation, the figure shows that the Taylor rarefaction is relatively weaker than the oxyhydrogen case. In addition, the figure shows that the helium driver can achieve a perfectly-driven condition. Therefore, it can be concluded that the shock-induced detonation may approach the perfectly-driven mode, when (*i*) a light gas is used as the driver gas, (*ii*) the initial driver pressure and temperature are high, (*iii*) the post-detonation pressure is low, and (*iv*) a_{CJ} and u_{CJ} are small.

It is difficult to determine the experimental plateau pressure $\bar{p}_{400}$. Thus, the pressures are averaged over a certain time before the reflected shock arrives at PT_4. This averaging time is arbitrary, but 0.25 ms is selected with careful consideration of the reflected shock and strong Taylor rarefaction. For the experiments with oxyhydrogen reactants at $p_{100} = 1.99$–2.01 atm, $\bar{p}_{400}$ is shown as solid squares with a one standard deviation error bar in Fig. 11. The trend of the experimental values being lower than the theoretical line implies that the Taylor rarefaction is stronger than theoretical predictions. This is possibly due to the low pressure in the double diaphragm section which abruptly reduced the actual pressure in the driver when the diaphragm is ruptured. Nonetheless, this discrepancy is within the data uncertainty.

For the same detonation mixture and initial conditions as those shown in Fig. 7 but with a helium driver, Fig. 12 shows nearly perfectly-driven pressure traces. Also, the theoretical p_{CJ} and p_{400} show good agreement with the experimental results. The reflected shock in Fig. 12 produces a much higher pressure than with an air driver. After the reflected shock, the pressure does not decrease but even increases due to blowdown of the high-pressure, driver tube gas. The helium driver interface advances more than twice as fast as the air driver interface; $u_5 = 410$ m/s for the air driver and $u_5 = 860$ m/s for the helium driver. Using this speed, the location where the driver interface meets the reflected shock is estimated to be 0.29 m upstream of PT_5, which means that the reflected shock measured at PT_4 is propagating not through the detonated gas but through the helium expanded from the driver. In this case, p_{500} calculated using the previous method is no longer valid since the reflected shock speed is reduced as it encounters the helium at a lower temperature, that is, $a_5 < a_{400}$. Therefore, p_{500} denoted in Fig. 12 is somewhat underestimated.

Figure 13 shows the effect of the Taylor rarefaction on the measured $\bar{p}_{400}$. Circles and squares represent the experimental $\bar{p}_{400}$ when using air and helium drivers, respectively, with their standard deviations. A perfectly-driven detonation is indicated by the $p_{CJ} = \bar{p}_{400}$ line. Most detonations are under-driven while no over-driven conditions are achieved in the tests thus far. However, the figure illustrates that the helium driver could possibly eliminate the Taylor rarefaction better than the air driver. The figure also shows that there is room for improvement in the technique, as the under-driven mode may affect the constancy of the driven tube flow (Jiang et al., 1999, 2002).

5.6 Driven tube conditions

While there are limitations with the under-driven mode, it did provide an adequate amount of quasi-steady flow for an experimental program to measure the electrical conductivity of high-enthalpy gases seeded with alkali salts. This is illustrated by a comparison of an under-driven and a nearly perfectly-driven example. An example of detonation tube pressure histories for an under-driven condition is given in Fig. 14a. The detonation tube contains a stoichiometric oxyhydrogen mixture at an initial pressure of 1.5 atm, and the driver tube is pressurized to 219 atm with air. Time-of-flight measurements indicate a detonation wave propagation speed of 2920 m/s, which is almost identical to the theoretical CJ detonation wave speed for these conditions. For this under-driven mode, the incident detonation wave is followed by a Taylor rarefaction that lowered the pressure. The reflected detonation wave in-

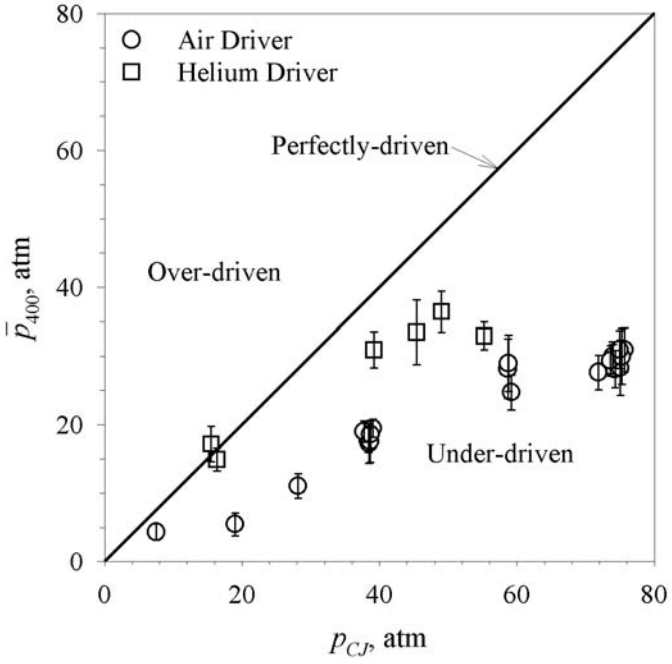

Fig. 13. Taylor rarefaction for air and helium driver

creases the pressure by a factor of 2.3, which agrees with CJ theory. However, the reduction in pressure caused by the rarefaction wave lowers the peak pressure behind the reflected detonation wave, although not nearly as much as observed for the arc-initiated detonation wave.

An example of a nearly perfectly-driven mode is shown in Fig. 14b, where the driver tube is filled with helium at 201 atm. The rate of pressure drop with time in this case is about the same as the previous example. However, the absolute pressure level achieved by the reflected detonation wave is much higher. This increase in reflected pressure increases the driven-tube Mach number from 6.70 to 7.65. (The highest peak shock Mach number achieved in the driven tube is 10.7.)

The corresponding pressure histories in the driven tube are shown in Fig. 15. The duration of quasi-uniform flow recorded by transducers PT_8 and PT_9, on either side of the test section, is at least 1 ms. Typically, the contact surface follows the shock wave after 0.76–0.79 ms. For a shock speed of the order of 300–400 m/s, this yields a 220–300 mm long slug of test gas. This length of test gas which is 2–3 times the conductivity channel is considered adequate for maintaining quasi-steady conditions for acquiring useful data.

5.7 Shock tube performance

Figure 16 shows the actual performance map of the shock tube. The abscissa and the ordinate represent the total pressure and temperature achieved in the driven tube. The steeply inclined lines represent different combinations of initial driver and detonation tube pressures. The driver gas is either helium or air, and the detonation tube is filled with a stoichiometric oxyhydrogen mixture, both initially at 300 K. The actual performance map is smaller than that shown in Fig. 2. One reason for this decrease is that the maximum driver tube pressure p_4 is held at 218 atm, instead of the maximum possible of 408 atm. Another reason is the initial reactant pressure p_{100} is limited to a maximum value of 3 atm, as the enthalpy conditions achieved are adequate for the tests under consideration. The widespread occurrence of under-driven conditions also limited the performance of the forward-propagating mode. Other reasons include boundary layer effects and gas cooling in both the detonation and driven tubes (Olivier et al., 2002). Nevertheless, the performance is sufficient for the test program and demonstrates the feasibility of using shock-induced detonation drivers for enhancing shock tube performance.

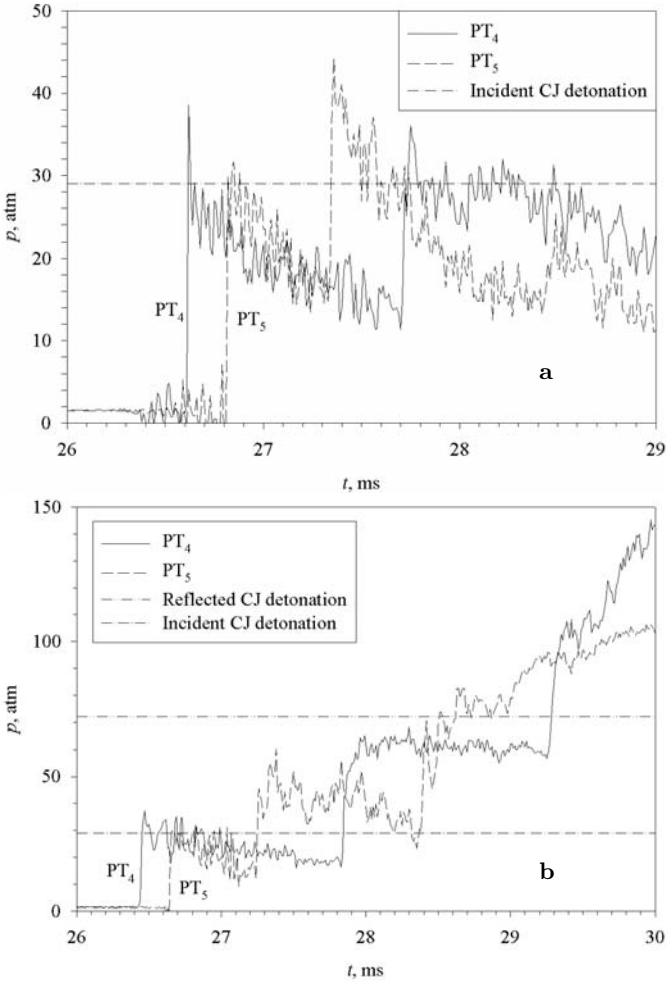

Fig. 14a,b. Detonation tube pressure traces for a stoichiometric oxyhydrogen mixture at an initial pressure of 1.5 atm with shock-induced detonation: **a** air driver (initial conditions of 219 atm and 300 K), **b** helium driver (initial conditions of 201 atm and 300 K)

6 Conclusions

A detonation-driven shock tube, operating in the forward mode, is described. The use of a driver tube to mitigate

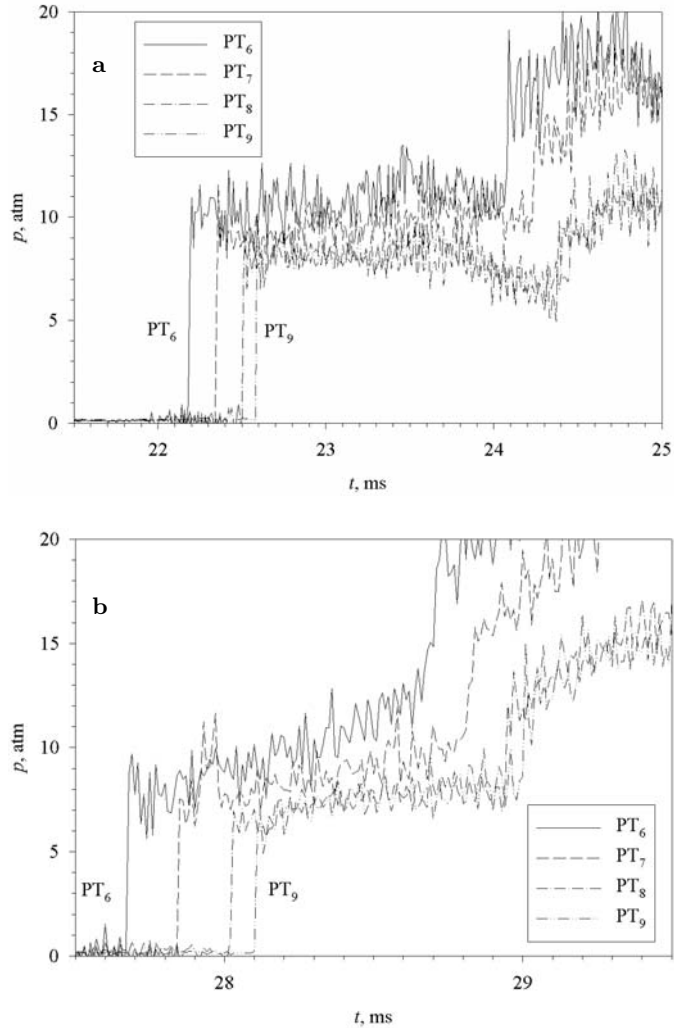

Fig. 15a,b. Driven tube pressure traces corresponding to Figs. 14a and b: locations PT_6–PT_9 are 2.146, 2.604, 3.061, 3.416 m downstream of diaphragm interface

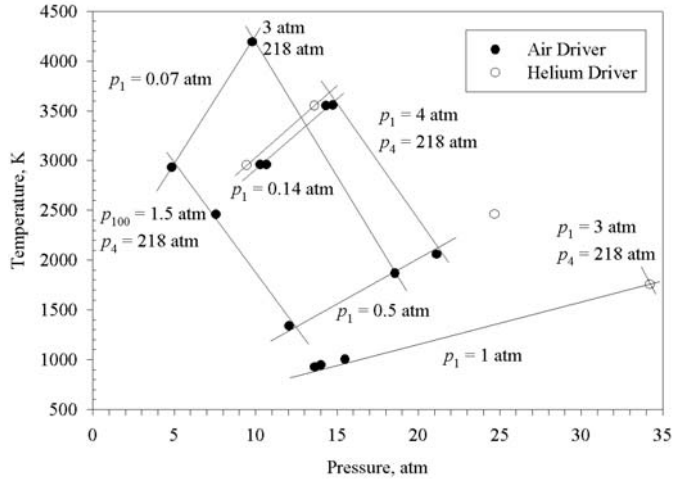

Fig. 16. Performance map of detonation-driven shock tube

the effect of the Taylor rarefaction yielded an adequate duration of uniform, high-pressure flow in the driven section compared to that achieved with an arc initiation. The performance of the shock tube is much lower than theoretical predictions. Possible reasons for the lower performance include shock attenuation in the driven tube, gas cooling in the detonation tube and poor fuel–oxidizer mixing. Nonetheless, the technique is found to be easy to implement. Air and helium at pressures of up to 408 atm were used to initiate a detonation wave in various fuel–oxidizer mixtures at pressures of up to 3 atm. A stagnation temperature of up to 4200 K and a stagnation pressure of up to 34 atm were achieved in air, initially at 1–2 atm.

Acknowledgements. The authors acknowledge the help of K.R. Burge, J.H. Holland, H.-C. Liu, C.H. Kim and W.S. Stuessy with the experiments. We are indebted to R.J. Bakos and J.I. Erdos of GASL, Ronkonkoma, New York, for many helpful discussions concerning the shock-induced detonation mode of operation, and to G. Emanuel for discussions on confined gaseous detonations. The detonation driven facility was developed partly with funding from MSE, Inc., Butte, Montana, through Contract No. 96-C323-F, monitored by Y.-M. Lee and G.A. Simmons, and by the Texas Advanced Technology Program under Grants 003656-056 and 003656-031.

References

Alpher RA, White DR (1958) Flow in shock tubes with area change at the diaphragm section. J Fluid Mech 3:457–470

Bakos RJ, Calleja JF, Erdos JI Sussman MA, Wilson GI (1996) An experimental and computational study leading to new test capabilities for the HYPULSE facility with a detonation driver. AIAA paper 96–2193

Bird GA (1957) A note on combustion driven shock tubes. AGARD Rep 146

Chue RSM, Tsai C-Y, Bakos RJ, Erdos JI, Rogers RC (2002) NASA's HYPULSE facility at GASL – a dual mode, dual driver reflected-shock/expansion tunnel. In: Lu FK, Marren DE (eds) Advanced hypersonic facilities. AIAA, Reston, Virginia, pp 29–71

Coates PB, Gaydon AG (1965) A simple shock tube with detonation driver. Proc Roy Soc A 283:18–21

Gordon S, McBride BJ (1976) Computer program for calculation of complex chemical equilibrium compositions and applications I. Analysis. NASA RP-1311 http://www.grc.nasa.gov/WWW/CEAWeb/xWhatCEA.htm

Hannemann K, Beck WH (2002) Aerothermodynamics research in the DLR high enthalpy shock tunnel HEG. In: Lu FK, Marren DE (eds) Advanced hypersonic facilities. AIAA, Reston, Virginia, pp 205–237

Itoh K (2002) Characteristics of the HIEST and its applicability for hypersonic aerothermodynamic and scramjet research. In: Lu FK, Marren DE (eds) Advanced hypersonic facilities. AIAA, Reston, Virginia, pp 239–253

Jiang Z, Yu HR, Takayama K (1999) Investigation into converging gaseous detonation drivers. In: Ball GJ, Hillier R, Roberts GT (eds) Proc 22nd Int Symp Shock Waves, Vol. 1. Imperial College, London, pp 527–532

Jiang Z, Wei Z, Chao W, Yu HR (2002) Study on high performance detonation-driven high enthalpy shock tunnels. In: Proc 23rd Int Symp Shock Waves, ed. by F.K. Lu, Univ Texas at Arlington, (CD-ROM)

Lu FK, Wilson DR, Bakos RJ, Erdos JI (2000) Recent advances in detonation techniques for high-enthalpy facilities. AIAA J 38(9):1676–1684

Morgan RG (2000) Development of X3, a superorbital expansion tube. AIAA paper 2000-0558

Nettleton MA (2002) Recent work on gaseous detonations. Shock Waves 12(1):3–12

Olivier H, Jiang Z, Yu H, Lu FK (2002) Detonation driven shock tubes and tunnels. In: Lu FK, Marren DE (eds) Advanced hypersonic facilities. AIAA, Reston, Virginia, pp 135–203

Stalker RJ (1967) A study of the free-piston shock tunnel. AIAA J 5(12):2160–2165

Thomas GO, Bambrey RJ (2002) Some observations of the controlled generation and onset of detonation. Shock Waves 12(1):13–21

Warren WR, Harris CJ (1970) A critique of high performance shock tube driving techniques. Shock Tubes. Proc 7th Int Shock Tube Symp, June 23–25, 1969, ed. by I.I. Glass, Univ Toronto Press, 143–176

Yu HR, Esser B, Lenartz M, Grönig H (1992) Gaseous detonation driver for a shock tunnel. Shock Waves 2(4):245–254